Faculty of physics

Institute for Quantum Information

Modeling of a nanomechanical oscillator with adiabatic correction to scattering theory

Bachelor Thesis
Felix Ihno Stamm
born in Osnabrück

Under supervision of Prof. Dr. Fabian Hassler and Dr. François Konschelle
Aachen, July 18, 2014

Acknowledgments

I would like to thank Prof. Dr. Hassler for the opportunity to write my bachelor thesis under his guidance. Further I would like to thank Prof. Dr.

Hassler and Dr. Konschelle for the countless interesting discussions and the supervision during the bachelor thesis.

I am also profoundly grateful to my parents which enable me to study here in Aachen and support me whenever I need it.

In addition, I would like to thank my girlfriend Christin Köhler for her support regardless of what I do.

For his immense support, I would like to thank Simon Schönebaum.

Last but not least, I would also like to thank Rania S. Baig, Kitlin Papa and many other students living in ESG-Aachen for their support.

Eidesstattliche Erklärung

Hiermit erkläre ich, Felix Ihno Stamm, an Eides statt, dass ich die vorliegende Bachelorarbeit selbständig verfasst und keine anderen als die angegebenen Quellen und Hilfsmittel benutzt habe.

July 18, 2014 _____

Felix Ihno Stamm

Contents

Introduction

Nanomechanical resonators or oscillators were recently studied in experiments [7, 9]. They consist of a shuttle installed on top of bridges or cantilevers. This shuttle is embedded in a measurement circuit and is resonant excited by another electrical circuit [6] or sonic waves [3]. Current through the measurement circuit is produced through mechanical transport of electrons on the shuttle. When the shuttle is close to the electron source, electrons tunnel onto the shuttle whereas they tunnel of the shuttle when the shuttle is close to the drain. Current induced due to this tunnel on, tunnel of process was already treated using a master-equation e.g. [5]. Thinking of the gaps between source/drain and the shuttle as potential barriers, resonant tunneling is another possibility for electron transport through the oscillator. We use a time-independent scattering approach to describe the resonant tunneling process through the oscillator at rest. To take into account the shuttle's slow motion, a separation of time scales is applied. Using the adiabatic expansion enables us to apply the results from the time-independent scattering approach to time-dependent problems.

Mesoscopic systems, such as the nanomechanical oscillator, allow the study of quantum effects on intermediary sized system, and quantum-transport therein has wide application in nanoeletronics. Consequently, it is of particular interest to study the motion of electrons, their quantum transport, through mesoscopic-circuits. Once these mesoscopic circuits contain moving mechanical parts, as the nanomechanical oscillator, modeling them requires the treatment of time-dependent problems.

Application of scattering concepts requires a separate treatment of an inner part, the scattering region (SR), and an outer part of the circuit(see fig. 1.1). The outer part consists of electron reservoirs (ER, e.g. voltage sources and measurement devices) and leads that connect the electron reservoirs to the scattering region. The outer region is treated classically whereas the scattering region is the mesoscopic part to study (the sample). As the sample is small in its size compared to the length of the leads, and the dwell time of an electron within the sample is considered small compared to the time resolution of the process, the electrons are considered coming in from $\pm\infty$ (in space) for time $t = -\infty$ and leaving to $\pm\infty$ for time $t = +\infty$. This concept proved very useful to describe electron transport and thereby also the current in time-independent mesoscopic-circuits.

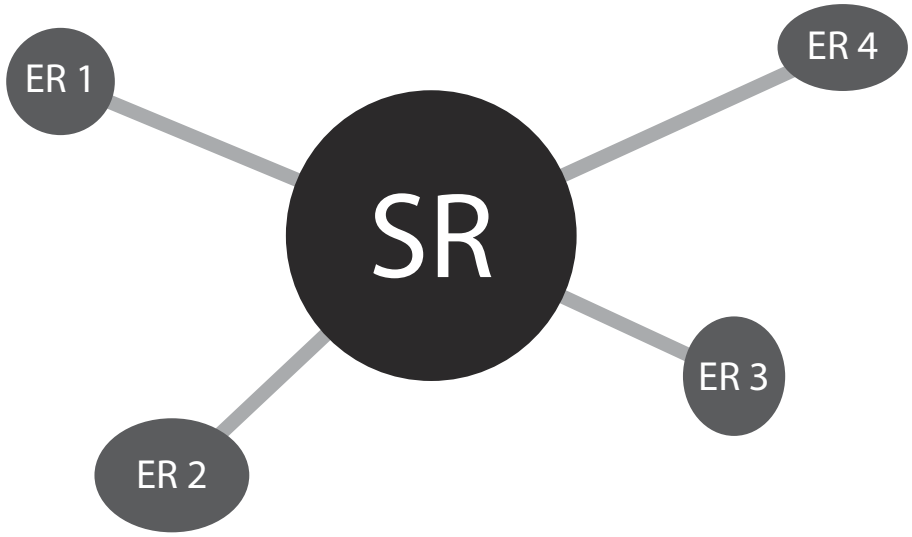

Figure 1.1: The basic scattering setup for mesoscopic-circuits, here with four electron reservoirs (ER). The dark gray regions indicate the electron reservoirs (ER) and the light gray lines display leads. All these objects belong to the outer region. The black central object is the scattering region (SR).

Using these scattering concepts that are designed for time independent samples, it is possible to describe mesoscopic-circuits coupled to mechanical oscillation. Thereby the basic idea is that the quantum-transport does happen so quickly that the sample did barely change while the electron is in the sample. This means that the oscillation period of the mechanical parts within the circuit is much larger then the dwell time of an electron within the scattering region. Using this assumption, we can approximate the time-dependent problem using the time-independent scattering approach. Goind beyond the instantaneous problem is called adiabatic expansion. It proved fruitful to describe backactions of the fast electrons on the slow mechanical motion as well as effects of the slow mechanical motion on fast moving electrons. Influence of the slow motion on the fast electrons, was treated e.g. by Moskalets and Büttiker[8]. Backactions of the electron flow (current) on the slow motion was treated e.g. by Thomas et al.[10].

In this work we use concepts of scattering and adiabatic expansion to model a nanomechanical oscillator (see. fig. 1.2). The scattering region for the oscillator consist of an island of fixed diameter and vanishing resistivity, the shuttle, embedded in a vacuum. We expect electrons to move freely within the shuttle whereas we expect them to tunnel through the vacuum. We assume that the mechanical motion for our system is a slow mechanical

oscillation of the shuttle.

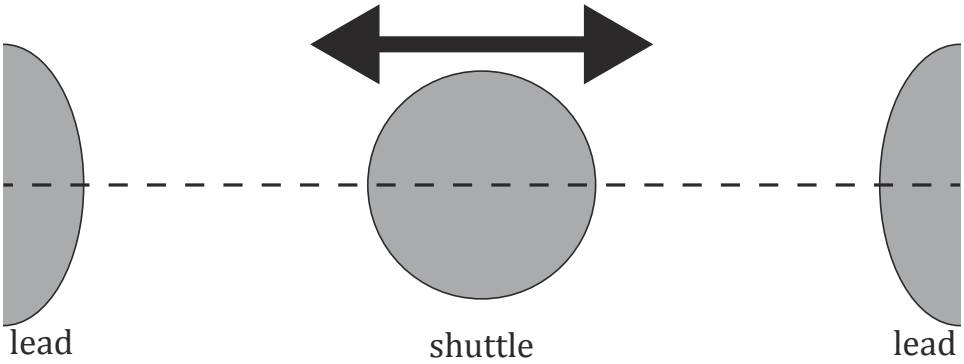

Figure 1.2: The nanomechanical oscillator with ideal leads on each side, which are connected to the rest of the circuit. Gray regions indicate conducting components and allow for free electron movement. White regions indicate a high resistivity which restricts the electron's movement. The shuttle in the center is slowly oscillating back and forth.

Resonant tunneling is already present in a one dimensional model. Therefore for simplification the oscillator is modeled as a 1D mesoscopic sample. This means, that we concentrate on the dashed line in fig. 1.2.

In this work we will firstly use time-independent scattering theory to understand quantum transport through the oscillator. Secondly, we use the adiabatic expansion up to first order to model the shuttle's movement. To calculate both the zeroth and first order we only need to solve the time-independent scattering problem and treat it with time-dependent parameters [8].

We begin with an introduction to the stationary scattering matrix $\mathbf{S}$, the main object used in time-independent(stationary) scattering theory.
Throughout the next subsections, we step by step model the nano-mechanical oscillator coupled to electronic reservoirs. To this end, we first calculate the scattering matrix of a rectangular barrier. This barrier is treated in a tunneling limit in the following subsection in more details. We will then make use of a composition law for scattering matrices to model the shuttle embedded in the insulator sea. Closing section 1, resonances originating from quantum interference are studied.

The second section deals with effects of the shuttle's motion using the adiabatic expansion. Firstly the idea of adiabatic expansion for our setup is outlined. In the following sections we will obtain the zeroth order correction the $\mathbf{S}_t$-matrix and the first order correction strength matrix $\mathbf{A}_t$.

Scattering Theory

Before we can discuss effects of the shuttles's slow motion, it is essential to understand the physics for the time-independent oscillator. Further more, we will see in section 3 that the results obtained for the time-independent oscillator can be used to make predictions for the slowly moving shuttle.

As we want to study quantum effects of electrons moving through the oscillator we will consider the oscillator as a mesoscopic sample that is connected with two ideal leads (see Fig. 1.2) on both sides. These ideal leads are both connected to different electron reservoirs.

For simplification, we consider these leads to be small in their size in y and z directions whereas the leads should be long in x direction. Hence, we can neglect the influence of propagation modes in y and z direction and deal only with movement in x direction. The transverse modes are referred to as "channels". Leads which are considered to have no such transverse modes are called single channel leads. We can see a sketch of a sample that is connected to two different single channel leads in Figure 2.1.

Figure 2.1: The basic scattering setup for a sample connected to two single channel leads. Further, there is an electron coming in through the left lead at time $t = -\infty$ but we cannot know whether the electron will leave the sample traveling to the right or traveling to the left for $t = +\infty$.

Due to the quantum nature of the interaction of electrons with the sample we cannot say whether each individual electron will be transmitted through the sample or whether it is back scattered. We can only make predictions in terms of probabilities for the electron's state after it has left the scattering region. These probabilities are used to predict the behavior of the sample when being connected to electron reservoirs. Some physical properties of

the sample depend only on the probabilities and properties that are further specifying the reservoirs. Others depend on the phase shift of a transition from incoming to outgoing states too (see e.g. section 3.2).

Scattering theory deals with the transition of incoming particles, which are in an incoming state for time $t = -\infty$, and the outgoing particles which are in an outgoing state for $t = +\infty$. The properties of transitions on large time scales from $t = -\infty$ to $t = +\infty$ are collected in the scattering matrix. To clarify: Information about the process for any finite time t is not included in the scattering matrix. Nevertheless the scattering matrix is a central element of scattering theory and many properties of the sample could be obtained with its help.

For our time-independent 1D single channel problem (time-independent oscillator) there are only two possible incoming states (+ states) for fixed energy. These represent an electron coming in through the left (see Fig. 2.1) or through the right lead. In addition, there are only two possible outgoing states (− states) which are an electron leaving through the left or right lead. So for the 1D single channel problem there are four possible transitions. The properties of these transitions on the large time scale already discussed are combined in a two by two matrix, the scattering matrix or **S**-matrix.

The main properties of a 1D single channel scattering matrix are described in section 2.1. The scattering matrix for the oscillator is then obtained step by step throughout sections 2.2-2.5. We start with a single rectangular barrier as a model for high resistivity regions in section 2.2. This barrier is considered in a tunneling limit in section 2.2.1. Two scattering matrices, each modeling a single barrier in the tunneling limit, are used to model the entire oscillator in 2.4. We therefore make use of formulae for the combination of two scattering matrices which are derived in section 2.3. Finally, a resonance in the transmission probability for the oscillator is studied and a scattering matrix for further study of the resonance is developed in section 2.5.

2.1 The S-matrix

We will discuss time-independent scattering theory, especially the scattering matrix, in 1D with two leads, each with a single scattering channel. We follow notation from[10].

The system of interest should be described by a single particle Hamiltonian $H_X = H_0 + V_X$ with a free particle Hamiltonian $H_0 = \frac{p^2}{2m}$ where m is the mass of the particle. We are especially considering electrons. In particular, the potential V_X is dependent on a parameter X so that the potential in position space $V_X(x)$ is fixed for all x when specifying this parameter. As the sample should be of finite size we would expect the potential to vanish

outside a finite region. Outside this region the free particle Hamiltonian describes the movement of the electron within the leads. As the Hamiltonian is time independent we can reduce the time dependent Schrödinger Equation to the time independent Schrödinger Equation (2.1). In this way we also properly defined the energy E. From all solutions to the time independent Schrödinger-Equation

$$(H_0 + V(X))\,|\Psi^{+/-}_{R/L\,X}\rangle = E\,|\Psi^{+/-}_{R/L\,X}\rangle \tag{2.1}$$

we concentrate on two different basis sets (+, −) each with two (R/L) basis states $|\Psi^{+/-}_{R/L\,X}\rangle$. The states are considered for energy E unless otherwise stated. The subscripts R/L correspond to the direction of propagation whereas the superscripts $+/-$ indicate whether we are dealing with a state before (+) or after (−) the scattering.

To further specify the basis sets we consider the eigenstates $|\phi_{R/L}(E)\rangle$ of the free Hamiltonian H_0 which fulfill

$$H_0\,|\phi_{R/L}\rangle = E\,|\phi_{R/L}\rangle\,. \tag{2.2}$$

The basis states with non-vanishing potential $|\Psi^{+/-}_{R/L\,X}\rangle$ are related to the eigenstates of the free Hamiltonian $|\phi_{R/L}\rangle$ via the Lippmann-Schwinger Equation

$$|\Psi^{+/-}_{R/L\,X}\rangle = |\phi_{R/L}\rangle + G^{+/-}_X V_X\,|\Psi^{+/-}_{R/L\,X}\rangle\,. \tag{2.3}$$

If the free eigenstates are normalized so that $\langle\phi_m(E')|\phi_n(E)\rangle = 2\pi\delta_{mn}\delta(E'-E)$ with m,n=R/L the $|\Psi^{+/-}_{R/L\,X}\rangle$ are normalized in the same manner. The retarded (+) or advanced (−) Greens function $G^{+/-}$ in the Lippmann-Schwinger Equation is

$$G^{+/-} = \lim_{\eta\to 0^+} \frac{1}{E - H_X \pm i\eta}. \tag{2.4}$$

According to the Green's function the scattering states are also called retarded (+) or advanced (−) scattering states. The retarded or advanced Green's functions correspond to the different boundary conditions[10]. We will see this property when discussing scattering in position space. We are now able to define the time independent scattering matrix $\mathbf{S}_X$.

$$2\pi\delta_{nk}\delta(E'-E)\mathbf{S}_X = \begin{pmatrix} \langle\Psi^-_{L\,X}(E')|\Psi^+_{R\,X}(E)\rangle & \langle\Psi^-_{L\,X}(E')|\Psi^+_{L\,X}(E)\rangle \\ \langle\Psi^-_{R\,X}(E')|\Psi^+_{R\,X}(E)\rangle & \langle\Psi^-_{R\,X}(E')|\Psi^+_{L\,X}(E)\rangle \end{pmatrix} \tag{2.5}$$

We can see that the scattering matrix is a basis transformation from incoming (+) states to outgoing (−) states. As the probability for a transition from an incoming state to an outgoing state is the absolute value squared of the corresponding matrix element, the entries of the scattering matrix are the

probability amplitude of the corresponding incoming state ending up as the corresponding outgoing state. Further, the matrix elements also include the phase-shift originating from passing through the scattering region. Speaking of probabilities we would expect a conservation of particle. This means that the probabilities for all possible transitions from a single incoming state sum up to one. We find this main property of the scattering matrix in its unitarity

$$\mathbf{S}_X^\dagger \mathbf{S}_X = \mathbf{S}_X \mathbf{S}_X^\dagger = \begin{pmatrix} 1 & 0 \\ 0 & 1 \end{pmatrix}. \tag{2.6}$$

The diagonal terms of the resulting matrix ensure conservation of particle. The off diagonal terms ensure orthogonality of the states (R/L) within a basis set (+/−). We can show that the scattering matrix from Eq. (2.5) is unitary since the advanced states $|\Psi^-_{L/R\,X}\rangle$ and the retarded states $|\Psi^+_{L/R\,X}\rangle$ form an orthonormal basis for fixed X and energy E. See Appendix A for a detailed proof of the unitarity.

Let us now have a look at the scattering setup in position space. As we are considering potentials which are confined to a finite region for all X we can use Figure 2.2 to visualize the retarded and advanced scattering states. The illustration of the picture should be considered as an ansatz for the states outside of the scattering region. In particular, we would expect electrons to travel freely within the leads. Note that we make no predictions for the scattering region, considered and displayed as a black-box. The retarded scattering states only have a single particle incoming, whereas the advanced scattering states have only one outgoing particle.

It is often convenient to choose the basis for the ansatz as plane waves outside the scattering region. In position space these plane waves look like e^{ikx} (wave travelling to the right) or e^{-ikx} (wave travelling to the left) with $k = \frac{\sqrt{2mE}}{\hbar}$. As the plane waves are complex conjugate to each others, we find a relation between the retarded and advanced scattering states. An incoming state with initial propagation to the right(left) is the complex conjugate of an outgoing state with propagation to the left(right). This property is called time reversal symmetry and leads to the equality $\langle \Psi^-_{L\,X} | \Psi^+_{L\,X} \rangle = \langle \Psi^-_{R\,X} | \Psi^+_{R\,X} \rangle$. The scattering matrix $\mathbf{S}_X$ is then equal to its transpose $\mathbf{S}_X^T$.

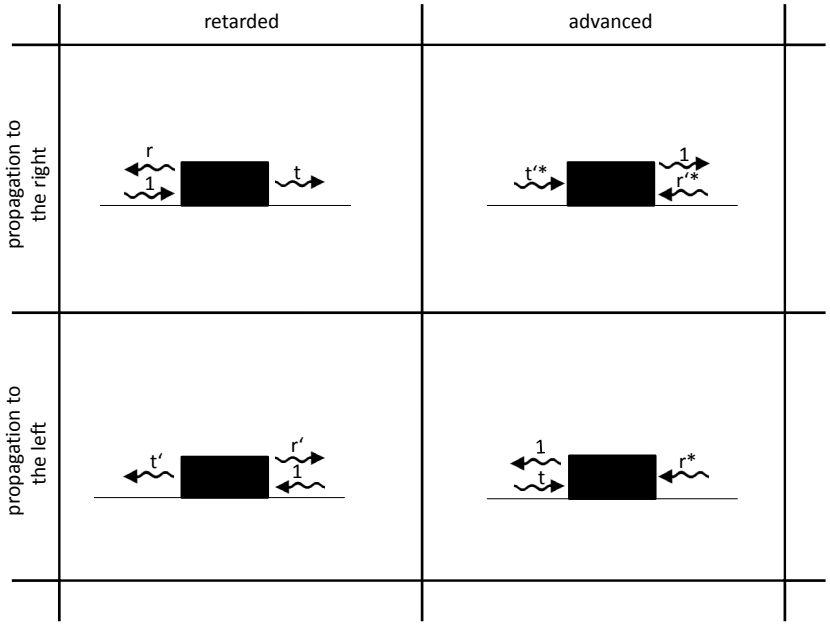

Figure 2.2: Visualization for the advanced and retarded scattering states. The black boxes indicate the scattering region with non vanishing potential. The retarded scattering have only one incoming wave with of the form $e^{\pm ikx}$ whereas the advanced scattering states have only outgoing waves of that form.

Matching the outgoing waves of retarded scattering states with outgoing waves of advanced scattering states, the retarded scattering states could be expressed in terms of the advanced scattering states. We find that with the ansatz from Figure 2.2

$$|\Psi^+_{RX}\rangle = t\,|\Psi^-_{RX}\rangle + r\,|\Psi^-_{LX}\rangle\,, \tag{2.7}$$
$$|\Psi^+_{LX}\rangle = r'\,|\Psi^-_{RX}\rangle + t'\,|\Psi^-_{LX}\rangle\,. \tag{2.8}$$

Inserting these equations into the definition of the scattering matrix Eq. (2.5) and using orthonormality of the scattering states we obtain the scattering matrix with respect to our ansatz

$$\mathbf{S}_X = \begin{pmatrix} r & t' \\ t & r' \end{pmatrix} = \begin{pmatrix} r & t \\ t & r' \end{pmatrix}. \tag{2.9}$$

In the following we will call all four entries of the scattering matrix $\mathbf{S}_X$ scattering coefficients. t, t' and r, r' are sometimes called transmission and reflection coefficient respectively. It is possible to further simplify the scattering matrix if the scattering potential $V_X(x)$ is symmetric with respect to

a point x_0. For such a symmetric problem the scattering process is the same regardless of whether considered from the left or from the right. This implies $r = r'$. For calculations with the scattering matrix it is useful to write the scattering coefficients in polar form. The scattering matrix would then show 8 degrees of freedom but the unitarity condition reduces the degrees of freedom to 4. The total number of degrees of freedom is further reduced by one for time reversal symmetry. So scattering matrices considered in 1D have three degrees of freedom. The polar form used here has three parameters θ, ϕ and $|t|$ and was adapted from[8]:

$$\mathbf{S}_X = e^{i\theta} \begin{pmatrix} e^{i\phi}\sqrt{1-|t|^2} & i\,|t| \\ i\,|t| & e^{-i\phi}\sqrt{1-|t|^2} \end{pmatrix} \tag{2.10}$$

This form of the scattering matrix is especially useful for calculations in section 3 but it is also used when making approximations of the scattering matrix. The phase ϕ encodes the asymmetry of the reflection from the right to the reflection from the left. If the symmetry $r = r'$ is given we find $\phi = 0$.

Finally, some special cases for the scattering matrix should be kept in mind. These special cases are frequently found as limits in more general cases. Given that the retarded and advanced scattering states are equal $|\Psi^-_{R/L\,X}\rangle = |\Psi^+_{R/L\,X}\rangle$ the $\mathbf{S}_X$-matrix simplifies to

$$\mathbf{S}_X = \begin{pmatrix} 0 & 1 \\ 1 & 0 \end{pmatrix}. \tag{2.11}$$

This means that a particle that starts traveling in one direction will end up traveling in the same direction after the scattering process. We can find this case for vanishing potential. On the other hand the scattering matrix is

$$\mathbf{S}_X = \begin{pmatrix} -e^{2ikL_{\text{left}}} & 0 \\ 0 & -e^{-2ikL_{\text{right}}} \end{pmatrix} \tag{2.12}$$

for vanishing transmission probability. Thereby, L_{left} and L_{right} indicate indicate the position of the divergence. A particle traveling in one direction (R/L) is leaving the scattering zone traveling in the other direction (L/R). Barriers of infinite height describe a setup where we find a scattering matrix in the form of Eq. (2.12).

2.2 Single rectangular barrier

We obtain the scattering matrix for a single rectangular barrier. The scattering matrix is defined in Eq. 2.5, to obtain it, we have to take care of the

phases as well as of the transmission amplitudes. The scattering matrix

$$\mathbf{S} = \begin{pmatrix} r & t \\ t & r \end{pmatrix} \tag{2.13}$$

for a single rectangular barrier is calculated. We have already used time reversal symmetry ($t = t'$) and the symmetry of the potential which results in $r = r'$. Note that we have dropped the dependency on a parameter X as used in section 2.1 for notational simplicity. To obtain the scattering matrix, wave functions $\Psi(x)$ which are solutions to the time independent Schrödinger equation

$$H\Psi(x) = E\Psi(x) \tag{2.14}$$

in position space are discussed and then the scattering matrix is obtained. The Hamiltonian in position space is $H = -\frac{\hbar^2}{2m}\partial_x^2 + V(x)$ with a piecewise constant potential

$$V(x) = \begin{cases} 0 & x \leq L_0 - \frac{w}{2} \\ V_0 & L_0 - \frac{w}{2} \leq x \leq L_0 + \frac{w}{2} \\ 0 & L_0 + \frac{w}{2} \leq x \end{cases} \tag{2.15}$$

where $V_0 > 0$ (see fig. 2.3). The barrier spans the space from $L_0 - \frac{w}{2}$ to $L_0 + \frac{w}{2}$.

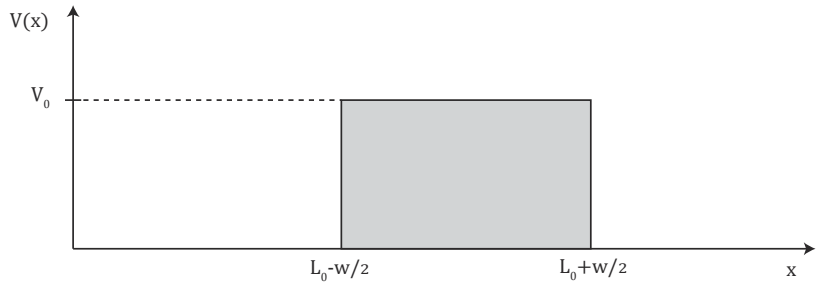

Figure 2.3: The piecewise constant potential $V(x)$ for a rectangular barrier.

In principle the scattering matrix is defined as a basis transformation from incoming states to outgoing states. For explicit calculations the ansatz presented in Figure 2.2 is widely used. We thus needn't calculate the basis transformation but we can use the scattering matrix from Eq. (2.9). So we start with a general solution of the Schrödinger equation (2.14) which for this potential is given as

$$\Psi(x) = \begin{cases} a_1 e^{ikx} + b_1 e^{-ikx} & x \leq L_0 - \frac{w}{2} \\ a_2 e^{-\rho x} + b_2 e^{\rho x} & L_0 - \frac{w}{2} \leq x \leq L_0 + \frac{w}{2} \\ a_3 e^{ikx} + b_3 e^{-ikx} & L_0 + \frac{w}{2} \leq x \end{cases} \tag{2.16}$$

where k and ρ are given as

$$k = \sqrt{\frac{2mE}{\hbar^2}} \tag{2.17}$$

$$\rho = \sqrt{\frac{2m(V_0 - E)}{\hbar^2}} = \sqrt{v^2 - k^2} = v\sqrt{1 - \left(\frac{k}{v}\right)^2}. \tag{2.18}$$

$v = \frac{\sqrt{2mV_0}}{\hbar}$ was defined according to V_0 as k to E. In the case $V_0 > E$ and $E > 0$ the parameters k, v and ρ are real. We make an ansatz for a retarded scattering state of the form

$$\Psi_R^+(x) = \begin{cases} e^{ik(x-L_0)} + re^{-ik(x-L_0)} & x \leq L_0 - \frac{w}{2} \\ A_-^R e^{-\rho x} + A_+^R e^{\rho x} & L_0 - \frac{w}{2} \leq x \leq L_0 + \frac{w}{2} \\ te^{ik(x-L_0)} & L_0 + \frac{w}{2} \leq x \end{cases} \tag{2.19}$$

which describes a wave incoming from the left which is reflected off the barrier with a reflection coefficient $r \in \mathbb{C}$ and is transmitted through the barrier with the transmission coefficient $t \in \mathbb{C}$. As the potential is finite for all x the wave function Ψ and its derivative with respect to x are expected to be continuous for all x. Matching $\Psi_R^+(x)$ and $\partial_x \Psi_R^+(x)$ at $x = L_0 - \frac{w}{2}$ and $x = L_0 + \frac{w}{2}$ results in the four linear equations for the four parameters r, t, A_+^R, A_-^R as function of the parameters k, ρ, w and L_0. From these equation we can find the transmission and reflection coefficient

$$t = e^{-ikw} \frac{\frac{4i\rho k}{(i\rho+k)^2} e^{-\rho w}}{1 - \frac{(i\rho-k)^2}{(i\rho+k)^2} e^{-2\rho w}}, \tag{2.20}$$

$$r = -e^{-ikw} \frac{\frac{i\rho-k}{i\rho+k}\left(1 - e^{-2\rho w}\right)}{1 - \frac{(i\rho-k)^2}{(i\rho+k)^2} e^{-2\rho w}} \tag{2.21}$$

$$\tag{2.22}$$

One can check that our scattering matrix is indeed unitary. For $E > V_0$ these formulae could also be found, and better understood using the Fresnel-equations together with the idea of multiple reflection from section 2.3. The Fresnel-equations describe the reflection and transmission of light passing from one medium into another with a different refractive index[4, p.238]. Using the wave-vectors k_1 and k_2 we can write the reflection (R_F) and transmission (T_F) probability obtained from the Fresnel-equations as

$$R_F = \left(\frac{k_1 - k_2}{k_1 + k_2}\right)^2 \tag{2.23}$$

$$T_F = \frac{4k_1k_2}{(k_1 + k_2)^2}. \tag{2.24}$$

Note that we only consider incoming light that hits the surface between the media at right angle. As the transmission or reflection probabilities are the same with k_1 and k_2 interchanged we can use the same reflection/transmission probability for the left or right end of the rectangular barrier. For the rectangular barrier the corresponding wave numbers are $i\rho$ and k.

As we know there are transmission and reflection resonances for multiple reflections. For $E > V_0 > 0$ and $i\rho L = n\pi$ ($n \in \mathbb{N}$) we find a transmission resonance with $|t| = 1$ whereas for $i\rho L = (n + 1/2)\,\pi$ we find local transmission minima. This is due to the multiple reflections between the edges of the potential barrier.

For tunneling processes with $V_0 > E > 0$ similar ideas apply. The probability reduction during the bouncing process is not happening due to $|r| < 1$ but rather due to the distance-traveled between the two ends of the barrier.

Other elementary properties of the scattering matrix could also be checked. We see that the scattering matrix is indeed independent of the position of the scattering potential L_0. Further, we find that making the substitution $\rho \approx ik$ which is equal to $V_0 \ll E$, the scattering matrix satisfies the high energy limit Eq. (2.11). For low energies $V_0 \ll E = v \ll k$ the scattering matrix assumes the form of Eq. (2.12).

2.2.1 The tunneling limit

Before we expand the scattering matrix for a single rectangular barrier in the tunneling limit there is one thing to keep in mind when expanding scattering matrices. Let us assume we have a scattering matrix $\mathbf{S}$ that is symmetric and depends on a small parameter ϵ. Expanding the scattering matrix with respect to the parameter ϵ ignoring terms of order n by simply expanding each element of the scattering matrix leads to a scattering matrix $\tilde{\mathbf{S}}$

$$\mathbf{S} = \begin{pmatrix} r & t' \\ t & r' \end{pmatrix} \approx \begin{pmatrix} \tilde{r} + O(\epsilon^n) & \tilde{t'} + O(\epsilon^n) \\ \tilde{t} + O(\epsilon^n) & \tilde{r'} + O(\epsilon^n) \end{pmatrix} = \tilde{\mathbf{S}} + O(\epsilon^n)\,. \tag{2.25}$$

The new "scattering matrix" $\tilde{\mathbf{S}}$ is unitary when dropping terms of order n. As the unitarity is very important, keeping this property while expanding should be a primary goal. The Büttiker representation of the scattering matrix (see. Eq. (2.10)) is very useful to achieve this goal. The unitarity of the scattering matrix is automatically upheld for all choices of the parameters $|t|$, θ and ϕ. So we try to expand the scattering matrix while keeping the unitarity. As the scattering matrix for the rectangular barrier fulfills $r = r'$ we find $\phi = 0$. Thus, it is sufficient to expand only one entry of the scattering matrix. The whole scattering matrix in that approximation is then calculated splitting the expanded entry into absolute value and phase factor.

As we are interested in tunneling processes, we would like to find a tunneling limit for the rectangular barrier from section 2.2. This means we want to consider only the primary tunneling process and no co-tunneling processes. This means we ignore tunneling paths which lead through the barrier more than ones. Therefor the transmission coefficient is considered for $\rho w \gg 1$ up to first order. We will consider the transmission coefficient for $kw \ll 1$ and $vw \gg 1$. These assumptions imply the usual tunneling limit $\rho w \gg 1$ and $\frac{k}{v} \ll 1$. We first expand the transmission coefficient from Eq. (2.20) for $\rho w \gg 1$ or equally setting the denominator equal to one as this means ignoring the longer paths. The transmission coefficient then is

$$t \approx \frac{4i\rho k e^{ikw} e^{-\rho w}}{(i\rho + k)^2}. \tag{2.26}$$

Now we expand for $\frac{k}{\rho} \ll 1$ which is equivalent to $\frac{k}{v} \ll 1$.

$$t \approx -4i\frac{k}{v} e^{ikw} e^{-vw} e^{\frac{1}{2}kw\frac{k}{v}} \tag{2.27}$$

Finally we use that $kw \ll 1$ and $\frac{k}{v} \ll 1$ which then leads to

$$t \approx -4i\frac{k}{v} e^{-vw}. \tag{2.28}$$

We can now use this approximated result for the transmission coefficient to calculate a unitary scattering matrix. We therefore split up the transmission coefficient into phase $ie^{i\theta} = -i$ and into absolute value $|t| = 4\frac{k}{v}e^{-vw}$. We can then use the Büttiker form from Eq. (2.10) with $\theta = \pi$ and $\phi = 0$ and find the unitary scattering matrix

$$\mathbf{S} = \begin{pmatrix} -\sqrt{1 - 16\left(\frac{k}{v}\right)^2 e^{-2vw}} & -4i\frac{k}{v}e^{-vw} \\ -4i\frac{k}{v}e^{-vw} & -\sqrt{1 - 16\left(\frac{k}{v}\right)^2 e^{-2vw}} \end{pmatrix}. \tag{2.29}$$

The scattering matrix describes the probability for the shortest and thus most likely tunneling path (thinking of Feynman path integrals again). In comparison with the scattering matrix for the rectangular barrier we have dropped both the phase information and longer tunneling paths.

2.3 Composition of two S-matrices

To model the shuttle setup we need to later on combine two scattering matrices to get a scattering matrix $\mathbf{S}_{12}$ describing the whole system. Obtaining the scattering matrix this way is sometimes a lot easier than matching the boundary conditions for the whole setup. (The same formulas could also

be obtained matching the boundary conditions.) It is further interesting to see that even though the modulus of the transmission coefficients of each single barrier might be small the resulting transmission amplitude of the double-barrier might be 1.

$$\mathbf{S}_{12} = \begin{pmatrix} r_{12} & t'_{12} \\ t_{12} & r'_{12} \end{pmatrix}. \tag{2.30}$$

Suppose the Hamiltonian in position space $H(x)$ is given as $H = H_0 + V_1(x) + V_2(x)$. The potentials $V_1(x)$ and $V_2(x)$ are supposed to be different from zero within an area of length w_1 and w_2 respectively. Further the two potentials are separated by an area of width L where $V(x) = V_1(x) = V_2(x) = 0$. So the entire potential which is also drawn in Figure 2.4 is given as

$$V(x) = \begin{cases} 0 & x \leq 0 \\ V_1(x) & 0 \leq x \leq w_1 \\ 0 & w_1 \leq x \leq w_1 + L \\ V_2(x) & w_1 + L \leq x \leq w_1 + L + w_2 \\ 0 & w_1 + L + w_2 \leq x \end{cases} \tag{2.31}$$

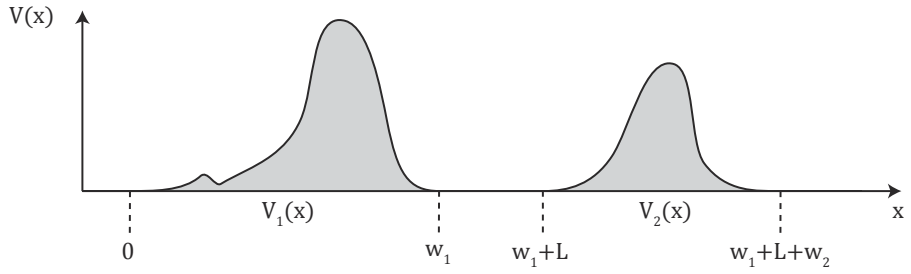

Figure 2.4: Potential $V(x)$ for a double barrier setup. The potential is non-vanishing for $0 \leq x \leq w_1$ where $V(x) = V_1(x)$ and for $w_1 + L \leq x \leq w_1 + L + w_2$ with $V(x) = V_2(x)$ only. The shape of both potentials $V_1(x)$ and $V_2(x)$ could be arbitrary.

We further use the the wave-vector

$$k = \frac{\sqrt{2mE}}{\hbar} \tag{2.32}$$

for regions with vanishing potential. Let us assume the scattering matrices $\mathbf{S}_1$ and $\mathbf{S}_2$ describing the scattering process at the single barriers $V_1(x)$ and

$V_2(x)$ are both transpose symmetric and of the form given in Eq. (2.10).

$$\mathbf{S}_1 = e^{i\theta_1} \begin{pmatrix} e^{i\phi_1}\sqrt{1-|t_1|^2} & i\,|t_1| \\ i\,|t_1| & e^{-i\phi_1}\sqrt{1-|t_1|^2} \end{pmatrix} \tag{2.33}$$

$$\mathbf{S}_2 = e^{i\theta_2} \begin{pmatrix} e^{i\phi_2}\sqrt{1-|t_2|^2} & i\,|t_2| \\ i\,|t_2| & e^{-i\phi_1}\sqrt{1-|t_2|^2} \end{pmatrix} \tag{2.34}$$

The scattering matrix $\mathbf{S}_{12}$ for the full potential $V(x)$ is entirely obtained in terms of the scattering coefficients of the single barriers and the length of the gab between the two. Instead of solving the Schrödinger equation for the two barriers the scattering matrix for the full system could also be obtained using a Feynman path integral concept. This means, we sum up all possible paths, weighted with their corresponding probability amplitudes, that the electron could have taken through the double barrier. This way we aim to find the scattering matrix for the full barrier.

To apply the Feynman path idea we will consider the electron as a wave. The amplitude of the wave corresponds to the square root of the corresponding probability. For the transmission amplitude we consider a wave coming in from the left. This wave is partly transmitted through the first barrier. The amplitude is reduced by $|t_1|$ and the wave acquires a phase shift $ie^{i\theta_1}$ (#1). It then travels a length L without reducing its amplitude but acquiring a phase shift e^{ikL} (#2).

By now there was only one path for the electron to get through the barrier. From here there are infinite many ways the electron could take to get to the other side of the barrier. Each path consists of zero or more bounces between the barriers before the electron is transmitted through the second barrier. For each bounce the wave is back scattered off the second barrier, acquiring a phase shift $e^{i(\theta_2+\phi_2)}$ and its amplitude is reduced by a factor $|r_2| = \sqrt{1-|t_2|^2}$. It then travels a distance L, acquiring a phase shift e^{ikL}, is reflected from the first barrier acquiring a phase shift $e^{i(\theta_1-\phi_1)}$ and its amplitude is reduced by $|r_2|$ before it acquires another phase shift e^{ikL} while traveling the distance L between the two barriers. The possible paths including up to 3 double-reflections are illustrated in Fig. 2.5.

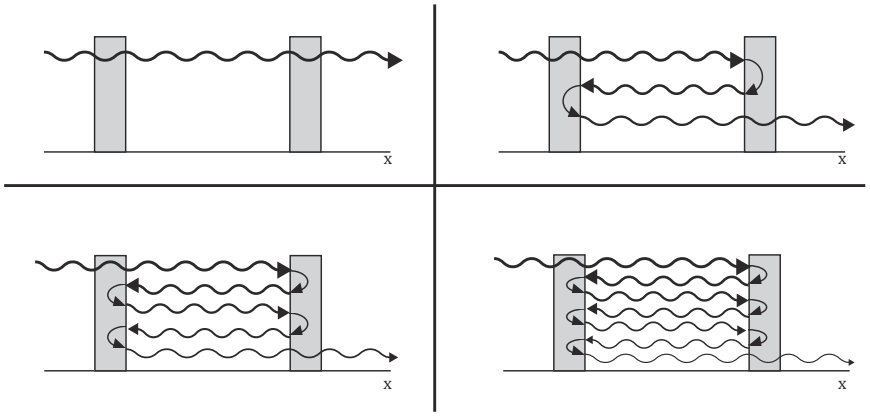

Figure 2.5: Possible electron paths for transmission through the double barrier setup. The barriers are indicated as gray boxes, their shape doesn't matter for this consideration. Top-left: no double reflection; top-right a single double-reflection; bottom-left: two double reflections; bottom-right: three double reflections.

This bouncing between the two potentials may happen up to an infinite amount of times (#3) but less and less probable. Finally after some bouncing between the two barriers part $|t_2|$ of the wave is transmitted through the second barrier acquiring a phase shift of $ie^{i\theta_2}$ (#4). All in all, the resulting transmission coefficient of the whole scattering process is

$$t_{12} = \underbrace{ie^{i\theta_1}\,|t_1|}_{(\#1)}\,\underbrace{e^{ikL}}_{(\#2)}\underbrace{\sum_{n=0}^{\infty}\left(e^{i(\theta_2+\phi_2)}\,|r_2|\;e^{ikL}\;e^{i(\theta_1-\phi_1)}\,|r_1|\;e^{ikL}\right)^n}_{(\#3)}\,\underbrace{ie^{i\theta_2}\,|t_2|}_{(\#4)}. \tag{2.35}$$

As the sum has an argument that has a modulus less then one we can use a geometric series identity to simplify the sum expression (#3).

$$\sum_{n=0}^{\infty}\left(e^{i(\theta_2+\phi_2)}\,|r_2|\;e^{ikL}\;e^{i(\theta_1-\phi_1)}\,|r_1|\;e^{ikL}\right)^n = \frac{1}{1-\left(e^{i(\theta_2+\phi_2)}\,|r_2|\,e^{ikL}e^{i(\theta_1-\phi_1)}\,|r_1|\,e^{ikL}\right)} \tag{2.36}$$

So the transmission coefficient is

$$t_{12} = -\frac{e^{i\theta_1}\,|t_1|\,e^{ikL}e^{i\theta_2}\,|t_2|}{1-\left(e^{i(\theta_2+\phi_2)}\,|r_2|\;e^{ikL}\;e^{i(\theta_1-\phi_1)}\,|r_1|\;e^{ikL}\right)}. \tag{2.37}$$

Next we will calculate the reflection happening to a wave coming from the left. When hitting barrier the left barrier part $|r_1|$ of the wave is reflected

acquiring a phase shift $e^{i(\theta_1+\phi_1)}$ whereas a part $|t_1|$ is transmitted through the potential 1 getting phase shifted by $ie^{i\theta_1}$. The wave then travels a distance L, is reflected of the second barrier's left side and then travels another distance L. The same bounce effect takes place as described above leading to the same infinite sum. This is only valid as we are considering a 1D problem with only one scattering channel. After the infinite bounce has taken place part $|t_1|$ is transmitted from the right through the first barrier being phase shifted by $ie^{i\theta_1}$. So the reflection coefficient of the whole setup is

$$r_{12} = e^{i(\theta_1+\phi_1)}\,|r_1| - \frac{e^{2ikL}\; e^{2i\theta_1}\,|t_1|^2\, e^{i(\theta_2+\phi_2)}\,|r_2|}{1-\left(e^{i(\theta_2+\phi_2)}e^{i(\theta_1-\phi_1)}e^{2ikL}\,|r_1|\,|r_2|\right)}. \tag{2.38}$$

In the same way we can get the reflection and transmission coefficients for a wave coming in from the right, being reflected with a reflection coefficient r'_{12} or being transmitted with a transmission coefficient t'_{12}.

$$r'_{12} = |r_2|\, e^{i(\theta_2-\phi_2)} - \frac{e^{2ikL}e^{i(\theta_1-\phi_1)}e^{2i\theta_2}\,|r_1|\,|t_2|^2}{1-\left(e^{i(\theta_2+\phi_2)}e^{i(\theta_1-\phi_1)}e^{2ikL}\,|r_1|\,|r_2|\right)} \tag{2.39}$$

$$t'_{12} = -\frac{e^{ikL}\,e^{i\theta_1}\,|t_1|\;e^{i\theta_2}\,|t_2|}{1-\left(e^{i(\theta_2+\phi_2)}e^{i(\theta_1-\phi_1)}e^{2ikL}\,|r_1|\,|r_2|\right)} \tag{2.40}$$

We simplify the expressions for the reflection coefficients using $\left|r_{1/2}\right|^2 + \left|t_{1/2}\right|^2 = 1$.

$$r_{12} = \frac{e^{i(\theta_1+\phi_1)}\,|r_1| - \left(e^{2i\theta_1}e^{2ikL}e^{i(\theta_2+\phi_2)}\right)|r_2|}{1-\left(e^{i(\theta_2+\phi_2)}e^{i(\theta_1-\phi_1)}e^{2ikL}\,|r_1|\,|r_2|\right)} \tag{2.41}$$

$$r'_{12} = \frac{e^{i(\theta_2+\phi_2)}\,|r_2| - \left(e^{2i\theta_2}e^{2ikL}e^{i(\theta_1+\phi_1)}\right)|r_1|}{1-\left(e^{i(\theta_2+\phi_2)}e^{i(\theta_1-\phi_1)}e^{2ikL}\,|r_1|\,|r_2|\right)} \tag{2.42}$$

Of interest to us is the resonance that appears when the bounce phase shift (see the phases in the denominators of the scattering coefficients) is equal to -1. This means the modulus of the transmission reaches the maximum value [1]. If we further consider two identical barriers (their probability amplitudes are identical) we find a pure transmission resonance with $|t_{12}|^2 = 1$. This implies that the reflection probability $|r_{12}|^2$ vanishes. This might seem quite strange considering the scattering scenario for a wave coming from the left which is partly reflected with an amplitude r_1 before really entering the scattering region. But it is no problem as we should not think of the wave traveling in time through the double barrier. We rather try to find all possible ways that lead to the same result.

To obtain the conditions that lead to the resonance we note that part $|r_1|$ is reflected off the first barrier but the reflection coefficient of the whole barrier vanishes so there has to be some annihilating part. Let us therefore consider

the part that is transmitted through the first barrier. After the transmission it travels freely, it is reflected off the second barrier, travels freely again and is transmitted through barrier 1 from the right side. The whole phase shift this part of the wave acquires is $-e^{2i\theta_1}e^{i(\theta_2+\phi_2)}e^{2ikL}$ whereas the reflected part acquired a phase shift of $e^{i(\theta_1+\phi_1)}$ only. For destructive interference they have to be anti-parallel which leads to

$$-e^{2i\theta_1}e^{i(\theta_2+\phi_2)}e^{2ikL} = -e^{i(\theta_1+\phi_1)}. \tag{2.43}$$

We left out that part of the wave that is reflected off the right end of the first barrier and thus begins the infinite bounce. This part initially has the same phase shift as the one mentioned above but acquires more with each double reflection. For destructive interfere with the initially reflected wave the further acquired phase shift has to be one (compare equation (2.36)). So the second equation for perfect transmission is

$$e^{2ikL}e^{i(\theta_1-\phi_1)}e^{i(\theta_2+\phi_2)} = 1. \tag{2.44}$$

Even though the equations (2.43) and (2.44) were obtained using different approaches these two equations are equivalent.

For a resonance with transmission probability one the amount of probability lost in one bounce round between the two barriers has to be equally distributed between the left and right side of the whole barrier. We can then think of the probability on the left side is "stolen" and transferred to the right side with each double reflection. In the end, the entire probability is confined to the right side of the barrier.

When the phase shift $e^{2ikL}e^{i(\theta_1-\phi_1)}e^{i(\theta_2+\phi_2)}$ is not precisely 1 a phase shift of $\Delta\alpha$ is acquired with each bounce. So after a finite number $N = \frac{\pi}{\Delta\alpha}$ of bounces from the left to right, the part that first interfered constructively (destructively) will then start to interfere destructively (constructively). After another N bounces the effect is shifted again. So the total transmission coefficient drops when the resonance condition Eq. (2.44) is no longer fulfilled. For low transparency $\left|t_{1/2}\right|^2 \approx 0$ we find that (far) away from the resonant case the transparency is almost vanishing $t_{12} \approx |t_1|\,|t_2| \approx 0$, whereas in the resonant case the transmission coefficient t_{12} might even become 1.

Finally, there is left to say that similar formulas could be obtained for a constant potential between the two potential barriers. Therefor you have to take care of the transition from one scattering potential to the constant potential as the scattering matrices expect free propagation on both sides.

2.4 Two Rectangular Barriers

Obtaining the formulas describing the shuttle is done straightforwardly using section 2.3. The scattering matrices for each single barrier are considered in

the tunneling limit described in section 2.2.1. We assume that the left/right barrier has width w_1/w_2 and that both are of height V_0. The gap between the two is of width L. The scattering coefficients for the double barrier system are then given as

$$r_{12} = \frac{e^{2ikL}\sqrt{1-16\left(\frac{k}{v}\right)^2 e^{-2vw_2}} - \sqrt{1-16\left(\frac{k}{v}\right)^2 e^{-2vw_1}}}{1-e^{2ikL}\sqrt{1-16\left(\frac{k}{v}\right)^2 e^{-2vw_1}}\sqrt{1-16\left(\frac{k}{v}\right)^2 e^{-2vw_2}}} \tag{2.45}$$

$$r'_{12} = \frac{e^{2ikL}\sqrt{1-16\left(\frac{k}{v}\right)^2 e^{-2vw_1}} - \sqrt{1-16\left(\frac{k}{v}\right)^2 e^{-2vw_2}}}{1-e^{2ikL}\sqrt{1-16\left(\frac{k}{v}\right)^2 e^{-2vw_1}}\sqrt{1-16\left(\frac{k}{v}\right)^2 e^{-2vw_2}}} \tag{2.46}$$

$$t_{12} = t'_{12} = -\frac{16\frac{k^2}{v^2}e^{ikL}e^{-v(w_1+w_2)}}{1-e^{2ikL}\sqrt{1-16\left(\frac{k}{v}\right)^2 e^{-2vw_1}}\sqrt{1-16\left(\frac{k}{v}\right)^2 e^{-2vw_2}}} \tag{2.47}$$

The scattering matrix associated with these scattering coefficients is indeed unitary.

2.5 Resonance for two rectangular barriers

As already pointed out in section 2.3 we can find a resonant behavior for a composed scattering matrix if the resonance condition (2.44) is fulfilled. For the setup of two rectangular barriers the resonance condition is independent of the parameters of the two barriers and simplifies to

$$kL = n\pi, \tag{2.48}$$

with n a positive integer. The behavior near the first resonance at $kL = \pi$ is investigated. Similar results are obtained for the other resonances. The analysis of the scattering matrix is conducted in terms of the three independent parameters $|t_{12}|$, ϕ and θ in the Büttiker representation Eq. (2.10). We will start by obtaining an expression for $|t_{12}|$ and $e^{i\theta} = {}^{t_{12}}/_{|t_{12}|}$ from an approximated transmission coefficient t_{12}. The the analysis is conducted in terms of the reflection coefficients $|t_1| = 4{}^{k}/_{v}e^{-vw_1} \ll 1$ and $|t_2| = 4\frac{k}{v}e^{-vw_2} \ll 1$ we

already encountered when dealing with the single barriers.

$$t_{12} = -\frac{e^{ikL}\,|t_1|\,|t_2|}{1-(e^{2ikL}+1-1)\sqrt{1-|t_1|^2}\sqrt{1-|t_2|^2}} \tag{2.49}$$

$$= -\frac{e^{ikL}\overbrace{\frac{|t_1|\,|t_2|}{1-\sqrt{1-|t_1|^2}\sqrt{1-|t_2|^2}}}^{=t_{res}}}{1-(e^{2ikL}-1)\underbrace{\frac{\sqrt{1-|t_1|^2}\sqrt{1-|t_2|^2}}{1-\sqrt{1-|t_1|^2}\sqrt{1-|t_2|^2}}}_{=\frac{1}{2}\alpha t_{res}}} \tag{2.50}$$

We defined the width of the resonance for a symmetric barrier as $\alpha(k)$. We will see that we can consider α to be independent of k. With $kL = \pi$, t_{res} describes the drop of the maximum value with the asymmetry of the barrier. As we assumed that $e^{-vw_{1/2}} \ll 1$ and $k \ll v$ we can simplify the expressions involving $t_{0,1/2} \propto e^{-vw_{1/2}} \ll 1$. We will first apply these approximations to t_{res}.

$$t_{res} = \frac{|t_1|\,|t_2|}{1-\sqrt{1-|t_1|^2}\sqrt{1-|t_2|^2}} \approx \frac{|t_1|\,|t_2|}{1-\left(1-\frac{1}{2}|t_1|^2\right)\left(1-\frac{1}{2}|t_2|^2\right)} \tag{2.51}$$

$$\approx \frac{|t_1|\,|t_2|}{\frac{1}{2}\left(|t_1|^2+|t_2|^2\right)} = \frac{1}{\cosh(2va)} \tag{2.52}$$

In the last step the definitions of $t_{0,1/2}$ were used and the whole system was parametrized in terms of an antisymmetry parameter a and the total length of the barriers $L_0 = w_1 + w_2$ (see Fig. 2.6).

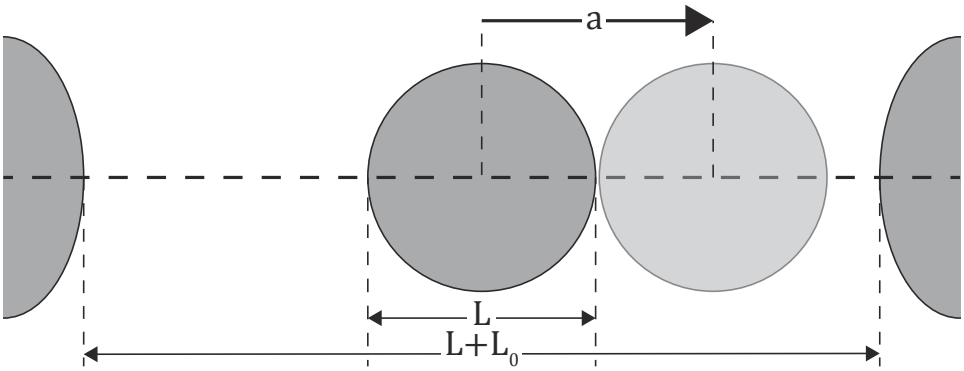

Figure 2.6: Nanomechanical oscillator with the parameters a and L_0.

The antisymmetry parameter a allows for a motion of the shuttle as $2a$ is the length difference of the two barriers. Keeping L_0 fixed changing a enlarges one barrier while the other one shrinks. The lengths of the two individual barriers are then given as

$$w_1 = \frac{L_0}{2} + a \tag{2.53}$$

$$w_2 = \frac{L_0}{2} - a \tag{2.54}$$

$a = 0$ corresponds to two barriers of equal length which then leads to a resonance with $|t_{12}| = 1$ for $kL = \pi$. For $a > 0$ ($a < 0$) the first (second) barrier is longer than the second (first) one. The restrictions on $w_{1/2}$ imply the following relations $vL_0 \gg va \gg 1$ for the new parameters of our system. We can also use the tunneling limit to simplify $1/2\alpha(k)t_{res}$.

$$\frac{1}{2}\alpha(k)t_{res} = \frac{\sqrt{1-|t_1|^2}\sqrt{1-|t_2|^2}}{1-\sqrt{1-|t_1|^2}\sqrt{1-|t_2|^2}} \approx \frac{1+\frac{1}{2}\left(|t_1|^2+|t_2|^2\right)}{\frac{1}{2}\left(|t_1|^2+|t_2|^2\right)} \tag{2.55}$$

$$\approx \frac{1}{\frac{1}{2}\left(|t_1|^2+|t_2|^2\right)} = \frac{\frac{1}{16}\frac{v^2}{k^2}e^{vL_0}}{\cosh(2va)} \tag{2.56}$$

$$\Rightarrow \alpha(k) = \frac{2}{16}\frac{v^2}{k^2}e^{vL_0} \tag{2.57}$$

As the dependency of $\alpha(k)$ on k is not very strong, we define α close to $k = \pi/L$

$$\alpha = \frac{2}{16\pi^2}L^2v^2e^{vL_0}. \tag{2.58}$$

We see that α is exponentially large because the tunneling limit implies $vL_0 \gg 1$. It is now possible to rewrite t_{12} close to $k = \pi/L$ in terms of α and t_{res}.

$$t_{12} \approx \frac{e^{ikL}t_{res}}{1-i\left(kL-\pi\right)\alpha t_{res}} \tag{2.59}$$

$$\Rightarrow |t_{12}| = \frac{t_{res}}{\sqrt{1+\left(kL-\pi\right)^2\alpha^2t_{res}^2}} \tag{2.60}$$

$$\Rightarrow e^{i\theta} = e^{ikL}\frac{\sqrt{1+\left(kL-\pi\right)^2\alpha^2t_{res}^2}}{1-i\left(kL-\pi\right)\alpha t_{res}} \tag{2.61}$$

As α is exponentially large, we find that the width of the resonance $\propto \alpha^{-2}$ is exponentially small on the kL-scale. Disregarding this sharpness we find

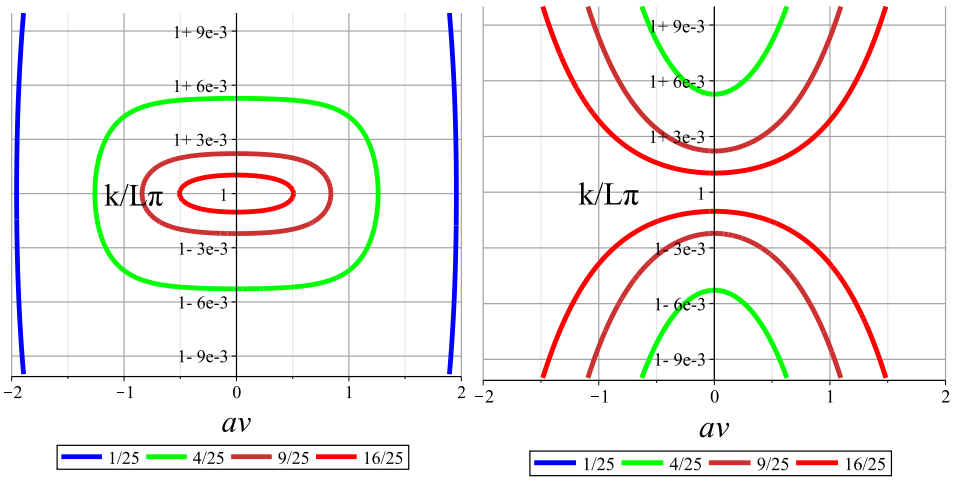

(a) Contour plot for $|t_{12}|$

(b) Contour plot for $|t_{12}|\cosh(2va)$

Figure 2.7: Resonance for resonant tunneling through two potential barriers (Eq. 2.60). Both plots (a) and (b) display the same choice of $\alpha = 1/8e^8$. (a) shows the resonance's shape whereas the broadening of the resonance with a is clearly visible in (b).

that the maximum value of $|t_{12}|$ for symmetric barriers ($a = 0$) remains the same as for symmetric barriers.

For asymmetric barriers the maximum value of the resonance shrinks exponentially with $|va|$ in its maximal height whereas the resonance broadens in terms of kL (see Fig. 2.7b). This broadening of the resonance leads to an a independent integral over k. The transmission coefficient as a function of av and $k/L\pi$ is displayed in Figure 2.7.

We can also see from Eq. (2.61) that the phase θ is well behaved close to the resonance. Using $e^{2i\phi} = \frac{r_{12}}{r'_{12}}$ we derive an expression $e^{2i\phi}$ for the phase

asymmetry of the reflection coefficients.

$$e^{2i\phi} = \frac{e^{2ikL}\sqrt{1-16\frac{k^2}{v^2}e^{-L_0 v}e^{+2va}} - \sqrt{1-16\frac{k^2}{v^2}e^{-L_0 v}e^{-2va}}}{e^{2ikL}\sqrt{1-16\frac{k^2}{v^2}e^{-L_0 v}e^{-2va}} - \sqrt{1-16\frac{k^2}{v^2}e^{-L_0 v}e^{+2va}}} \tag{2.62}$$

$$\overset{kL\approx\pi}{\approx} \frac{(1+i\,(kL-\pi))\sqrt{1-\frac{2}{\alpha}e^{+2va}} - (1-i\,(kL-\pi))\sqrt{1-\frac{2}{\alpha}e^{-2va}}}{(1+i\,(kL-\pi))\sqrt{1-\frac{2}{\alpha}e^{-2va}} - (1+i\,(kL-\pi))\sqrt{1-\frac{2}{\alpha}e^{+2va}}} \tag{2.63}$$

$$\overset{\alpha\gg1}{\approx} \frac{(1+i\,(kL-\pi))\left(1-\frac{1}{\alpha}e^{+2va}\right) - (1-i\,(kL-\pi))\left(1-\frac{1}{\alpha}e^{-2va}\right)}{(1+i\,(kL-\pi))\left(1-\frac{1}{\alpha}e^{-2va}\right) - (1+i\,(kL-\pi))\left(1-\frac{1}{\alpha}e^{+2va}\right)} \tag{2.64}$$

$$= \frac{-i\,(kL-\pi) + \frac{i(kL-\pi)}{\alpha}\cosh(2va) + \frac{1}{\alpha}\sinh(2va)}{-i\,(kL-\pi) + \frac{i(kL-\pi)}{\alpha}\cosh(2va) - \frac{1}{\alpha}\sinh(2va)} \tag{2.65}$$

$$\approx -\frac{-i\,(kL-\pi) + \frac{1}{\alpha}\sinh(2va)}{i\,(kL-\pi) + \frac{1}{\alpha}\sinh(2va)} \tag{2.66}$$

For the last approximation we dropped the terms that are small in both small quantities α^{-1} and $kL-\pi$. All approximations uphold $|r_{12}/r'_{12}| = 1$. This is necessary as r_{12}/r'_{12} should still represent the phase factor $e^{2i\phi}$. Note that for $a = 0$, $e^{2i\theta} = 1$ whereas for $kL = \pi$, $e^{2i\theta} = -1$. So $e^{2i\phi}$ is discontinuous at $kL = \pi$ and $a = 0$.

The adiabatic expansion

To describe the effect of the shuttle's movement on the physical system we would have to solve the time dependent Schrödinger equation. As the solution to the time dependent Schrödinger equation is hard to find we thus use the so called adiabatic expansion. The adiabatic expansion is an expansion of the exact result for the parametrically time dependent problem for small frequency of the motion. It uses a seperation of time-scales. The electrons' dwell time within the scattering region is consider very short compared to the shuttles oscillation period. To model the shuttles movement we will vary the antisymmetry $a = a(t)$. The adiabatic expansion then consists of an expansion in terms of time derivatives of the classical degree of freedom $a(t)$ [10].

We will consider only the zeroth and first order of this expansion. The frozen scattering matrix $\mathbf{S}_t$ is the zeroth order term in the expansion. In the zeroth order the time dependent system is that of the corresponding time-independent system with the same parameter a. The first order term $\dot{a}\mathbf{A}_t$ consists of the correction strength matrix $\mathbf{A}_t$ and time derivative $\partial_t a = \dot{a}$ of the oscillating parameter. With these two terms we can write the exact scattering matrix $\mathcal{S}$ as

$$\mathcal{S} = \mathbf{S}_t + \dot{a}\mathbf{A}_t + ... \tag{3.1}$$

3.1 The zeroth order ($\mathbf{S}_t$)

The zeroth order in the adiabatic expansion is the $\mathbf{S}_t$-matrix or frozen scattering matrix. The frozen scattering matrix $\mathbf{S}_t$ is the scattering matrix for the time independent problem where the classical degree of freedom a is now considered time dependent by setting $a = a(t)$. For the theory on the time independent problem see section 2.1.

To model the moving shuttle we will consider the scattering matrix obtained in section 2.5 which describes two rectangular barriers of equal height which are separated by a length of width L with vanishing potential. To model the movement of the shuttle we consider the asymmetry parameter a to be time dependent $a = a_0 \sin(\omega t)$.

3.2 The first order contribution ($\mathbf{A}_t$)

The first order term $\dot{a}\mathbf{A}_t$ in the adiabatic expansion was already defined in Eq. (3.1). It is possible to express the $\mathbf{A}_t$ matrix entirely in terms of the frozen scattering states [10]:

$$A_t^{nk} := \frac{\hbar}{2}\left(\langle\partial_E\Psi^-_{n\,a_t}|\partial_a V_t|\Psi^+_{k\,a_t}\rangle - \langle\Psi^-_{n\,a_t}|\partial_a V_t|\partial_E\Psi^+_{k\,a_t}\rangle\right) \tag{3.2}$$

where $|\partial_E\Psi^{+/-}_{n\,X}\rangle = \partial_E\,|\Psi^{+/-}_{n\,X}\rangle$ with $n = R/L$ denotes the derivative with respect to energy. The scattering states $|\Psi^{+/-}_{R/L\,X}\rangle$ were already introduced in section 2.1. ∂_a denotes the derivative with respect to the slowly varying parameter a.

A relation of the $\mathbf{S}_t$ and $\mathbf{A}_t$ was obtained through the unitarity of the scattering matrix[8, 2].

$$\mathbf{S}_t^\dagger\mathbf{A}_t + \mathbf{A}_t^\dagger\mathbf{S}_t = \frac{i\hbar}{2}\left(\partial_a\mathbf{S}_t^\dagger\partial_E\mathbf{S}_t - \partial_E\mathbf{S}_t^\dagger\partial_a\mathbf{S}_t\right) \tag{3.3}$$

If the frozen scattering matrix is symmetric, the $\mathbf{A}_t$ matrix is antisymmetric [8]. This means the first order adiabatic correction acts on the off-diagonal entries of the frozen scattering matrix. The scattering coefficients describing the reflection are left unchanged. So with the adiabatic correction the $\mathcal{S}$ matrix is no longer symmetric. It is very useful to use the Büttiker representation of the scattering matrix from Eq. (2.10). The antisymmetry of $\mathbf{A}_t$ also leads to an ansatz for the $\mathbf{A}_t$ matrix which fits with the scattering matrix from Eq. (2.10).

$$\mathbf{A}_t = e^{i\theta}\begin{pmatrix} 0 & \left(A_\perp + iA_\parallel\right) \\ -\left(A_\perp + iA_\parallel\right) & 0 \end{pmatrix}. \tag{3.4}$$

The parameter θ is defined in the generic scattering matrix Eq. (2.10). The parameters $A_\perp, A_\parallel \in \mathbb{R}$ are of further interest. The factor $A_\parallel$ is the strength of the correction on the transmission coefficient. Due to the ansatz, $A_\parallel$ and the transmission coefficient have the same phase. The parameter $A_\perp$ corresponds to a correction that is, thinking of complex number as vectors in the complex plane, orthogonal to the transmission coefficient. To further specify $A_\perp$ and $A_\parallel$ we use the unitarity condition from Eq. (3.3). With the general three parameter scattering matrix from Eq. (2.10) we find an expression for the left hand side of Eq. (3.3).

$$\mathbf{S}_t^\dagger\mathbf{A}_t + \mathbf{A}_t^\dagger\mathbf{S}_t = \begin{pmatrix} -2\,|t|\,A_\parallel & 2ie^{-i\phi}\sqrt{1-|t|^2}A_\parallel \\ -2ie^{i\phi}\sqrt{1-|t|^2}A_\parallel & 2\,|t|\,A_\parallel \end{pmatrix} \tag{3.5}$$

Note that $A_\perp$ is not part of the unitarity condition. The right hand side of Eq. (3.3) could also be calculated using the generic scattering matrix from Eq. (2.10). It resembles the structure of the left hand side.

$$\frac{i\hbar}{2}\left(\partial_a \mathbf{S}_t^\dagger \partial_E \mathbf{S}_t - \partial_E \mathbf{S}_t^\dagger \partial_a \mathbf{S}_t\right) = \hbar\left(\partial_E |t|\, \partial_a \phi - \partial_a |t|\, \partial_E \phi\right) \begin{pmatrix} -|t| & ie^{-i\phi}\sqrt{1-|t|^2} \\ -ie^{i\phi}\sqrt{1-|t|^2} & |t| \end{pmatrix} \tag{3.6}$$

It is now possible to solve for the parallel correction strength $A_\parallel$ in terms of derivatives of parameters of the scattering matrix.

$$A_\parallel = \frac{\hbar}{2}\left(\partial_E |t|\, \partial_a \phi - \partial_a |t|\, \partial_E \phi\right) = \frac{m}{2k\hbar}\left(\partial_k |t|\, \partial_a \phi - \partial_a |t|\, \partial_k \phi\right). \tag{3.7}$$

We can see that $A_\parallel$ is independent of the phase θ and does only depend on the derivatives of both the asymmetry of the reflection coefficients ϕ and the transmission probability amplitude $|t|$. This enables us to calculate the correction strength $A_\parallel$ for any two leads - single channel scattering matrix. As an example, the single rectangular barrier (see sec. 2.2) has vanishing $A_\parallel$. Nevertheless, we find a non-vanishing $A_\parallel$ for the double rectangular barrier. So we calculate $A_\parallel$ for the two barriers scattering matrix from section 2.5.

3.3 $\mathbf{S}_t$ and $\mathbf{A}_t$ for two rectangular barriers

The aim is to describe the physics of a moving shuttle. We therefore calculated the scattering matrix for a setup of two rectangular barriers of equal height with free space in between. See section 2.5 for further details and definition of the asymmetry parameter a. We will now consider the asymmetry parameter a to be time dependent (e.g. $a = a_0 \sin(\omega t)$). The time independent scattering matrix was already calculated in section 2.4 and approximated closely to the first resonance in sec. 2.5. We will use this approximated version of the scattering matrix. The frozen scattering matrix $S_{12,t}$ is obtained by setting $a = a(t)$.

To calculate the $\mathbf{A}_t$-matrix we can use Eq. (3.7) where the derivatives of $|t_{12}|$ are calculated straightforwardly as

$$\partial_k |t_{12}| = -L |t_{12}|^3 \alpha^2 (kL - \pi), \tag{3.8}$$

$$\partial_a |t_{12}| = -2v |t_{12}|^3 \sinh(2va) \cosh(2va). \tag{3.9}$$

Calculating the derivatives of ϕ we use

$$\partial_{k/a}\phi = \frac{1}{2i}\partial_{k/a} \ln\left(\frac{r_{12}}{r'_{12}}\right). \tag{3.10}$$

We calculate the derivatives of ϕ for the expression from Eq. (2.66)

$$\partial_k \phi = -\frac{L\alpha \sinh(2va)}{\alpha^2 (kL-\pi)^2 + \sinh(2va)^2}, \tag{3.11}$$

$$\partial_a \phi = 2\frac{v\alpha \cosh(2va)(kL-\pi)}{\alpha^2 (kL-\pi)^2 + \sinh(2va)^2}. \tag{3.12}$$

Note that these derivatives have a singularity at $kL = \pi$ and $a = 0$ which will get smoothed out if we multiply the derivatives of ϕ by those of $|t_{12}|$. Using all necessary derivatives we can calculate the correction strength $A_\parallel$.

$$A_\parallel = -\frac{mkvL\alpha}{\hbar} |t_{12}|^3 \cosh(2va) \tag{3.13}$$

$$A_\parallel \overset{kL\approx\pi}{\approx} -\frac{m\pi v\alpha}{\hbar} \frac{1}{\sqrt{1 + \frac{\alpha^2}{\cosh^2(2va)} (kL-\pi)^2}^3} \frac{1}{\cosh^2(2va)} \tag{3.14}$$

The correction strength is of similar shape as $|t_{12}|$. It is decreasing exponentially with $|av|$ to 0 and has a Lorentz-like shape in terms of kL centered around $kL = \pi$. Nevertheless, it is dropping quicker to zero with both av and kL. Further, the correction strength $A_\parallel$ is exponentially large because it is proportional α. The correction strength is visualized in Fig. Abb. 3.1a.

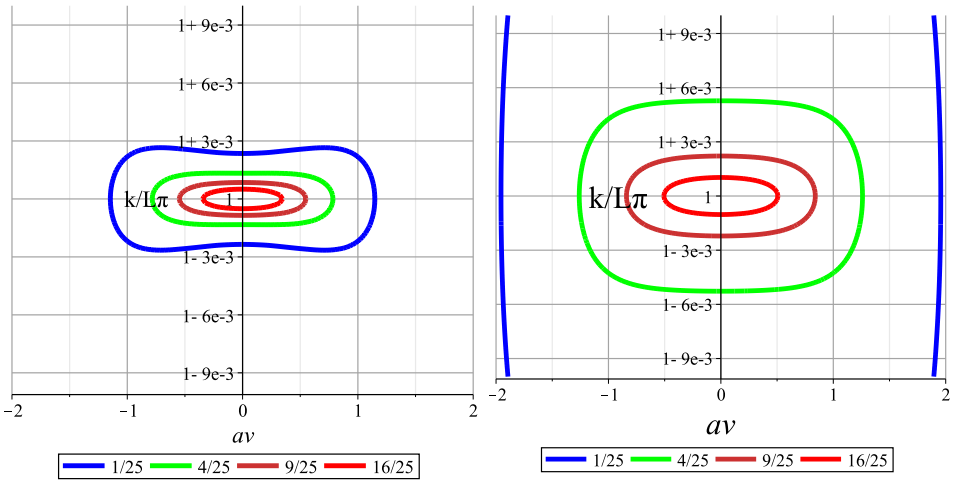

(a) Contour plot for $-\frac{\hbar}{m\pi v\alpha}A_{\|}$

(b) Contour plot for $|t_{12}|$

Figure 3.1: Both plots (a) and (b) display the same choice of $\alpha = 1/8e^8$. (a) shows $-\frac{\hbar}{m\pi v\alpha}A_{\|}$ and is thus a dimensionless visualization of $A_{\|}$ for comparison purposes t_{12} is visualized in (b).

The sign of $A_{\|}$ indicates that for $\dot{a} > 0$ tunneling from the left to the right is favored whereas tunneling from the left to the right is hindered. This effect is probably due to the shuttle approaching the right lead and thus shortening the gap. With a shorter gap tunneling off the island to the right lead is favored.

Conclusion

Resonant tunneling through a nanomechanical oscillator was studied. Starting with the scattering matrix for a single rectangular barrier, the tunneling limit was discussed and the scattering matrix accordingly approximated. Then two of these scattering matrices were combined to form a single scattering matrix that describes the tunneling process through a time-independent nanomechanical oscillator.

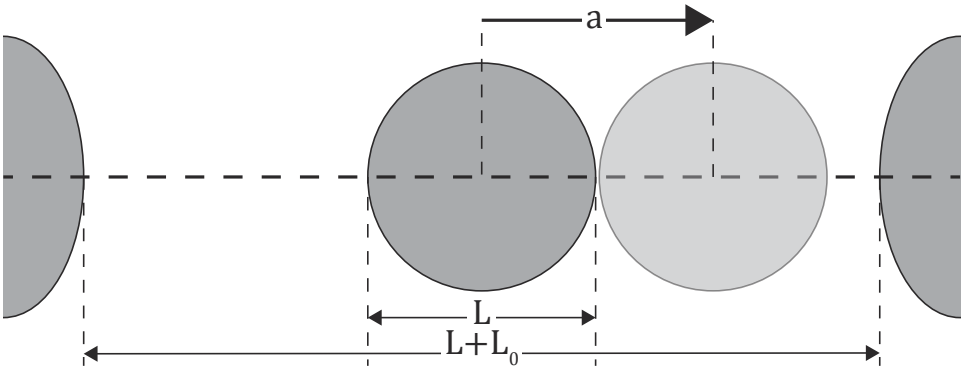

Figure 4.1: As can be seen in the center is a shuttle with the length L. Nanomechanical oscillator: In the center there is the shuttle of length L. To the left and right side are leads which are separated by a length of $L + L_0$. For the shuttle not being centered, the asymmetry parameter a is the displacement of the shuttle from the center.

Resonant tunneling for the time-independent nanomechanical oscillator was further discussed and a resonance condition was obtained. The resonance condition depends on two parameters: a) the wave-vector magnitude $k = \sqrt{2mE}/\hbar$ (with E being the energy of the incoming electron and m its mass), b) the length L of the shuttle. Further, the resonance with the smallest k at $kL = \pi$ was discussed. Close to the resonance the transmission probability $|t_{12}|^2$ is a Lorentz-function of kL; with a maximum value of one, under the condition of the shuttle being centered between the two leads. The Lorentz-function has exponentially small width for long and high barriers. Further, it decreases in its maximum height and broadens with the asymmetry a of the shuttle's position. Leading to the value of the transmission coefficient at $kL = \pi$ dropping exponentially with the asymmetry of a the shuttle's position between the two leads.

The following section focuses on the movement of the shuttle. To find an analytical solution, we used a separation of time scales. This means that, we assume that, the movement of the shuttle is relatively stagnant in comparison to the movement of the electrons through the oscillator. With this assumption we made an adiabatic expansion in terms of the slow motion of the shuttle. The zeroth order of the expansion: the $\mathbf{S}_t$-matrix is easily calculated replacing specific time-independent parameters within the time-independent scattering matrix with time-dependent parameters. The first order in the adiabatic expansion is $\mathbf{A}_t\dot{a}$ where $\mathbf{A}_t$ is an antisymmetric matrix and $\dot{a}$ is the time derivative of the slowly varying parameter $a(t)$. The correction strength matrix $\mathbf{A}_t$ has only one linearly independent entry: A. When considering complex numbers as vectors in the complex plane, the part of A that is parallel to the transmission coefficient of $\mathbf{S}_t$ was further discussed. For this parallel part $A_{\|}$ an expression in terms of the scattering matrix $\mathbf{S}_t$ was obtained. Finally, $A_{\|}$ was calculated for the nanomechanical shuttle.

We assume that the orthogonal part $A_{\perp}$ (corresponding to $A_{\|}$) of the correction strength does not influence the back actions of neither the electron flow on the shuttles' movement nor vice versa. With this assumption, both the scattering matrix $\mathbf{S}_t$ and the first order correction strength matrix $\mathbf{A}_t$ - presented in this work - could be used to calculate physical properties of the nanomechanical oscillator for various electron reservoirs and various movement patterns $a(t)$. These properties are either backactions of resonant tunneling electrons on the movement of the shuttle (the adiabatic reaction forces) or backactions of the shuttle's movement on the electron flow. In order describe these physical properties this report presents the first step, calculation of $\mathbf{S}_t$ and $\mathbf{A}_t$ for resonant tunneling through the nanomechanical oscillator, and leads to the next step, the calculation of adiabatic reaction forces or back-actions on the current. The adiabatic reaction forces are discussed in terms of $\mathbf{S}_t$ and $\mathbf{A}_t$ in a work by M. Thomas et al. [10]. Backactions on the electron flow are discussed by M. Moskalets and M. Büttiker [8] with a quite similar approach.

Appendix

To show the unitarity of the scattering matrix we start of with the definition of the scattering matrix in Eq. (2.5) and insert this definition into the left hand side of Eq. (2.6).

$$\begin{aligned}\mathbf{S}_X^\dagger \mathbf{S}_X &= \begin{pmatrix} \langle \Psi^+_{RX} | \Psi^-_{LX} \rangle & \langle \Psi^+_{RX} | \Psi^-_{RX} \rangle \\ \langle \Psi^+_{LX} | \Psi^-_{LX} \rangle & \langle \Psi^+_{LX} | \Psi^-_{RX} \rangle \end{pmatrix} \begin{pmatrix} \langle \Psi^-_{LX} | \Psi^+_{RX} \rangle & \langle \Psi^-_{LX} | \Psi^+_{LX} \rangle \\ \langle \Psi^-_{RX} | \Psi^+_{RX} \rangle & \langle \Psi^-_{RX} | \Psi^+_{LX} \rangle \end{pmatrix} \\ &= \begin{pmatrix} a_{11} & a_{12} \\ a_{21} & a_{22} \end{pmatrix},\end{aligned}$$

The entries a_{ij} are given as:

$$\begin{aligned} a_{11} &= \langle \Psi^+_{RX} | \underbrace{\left(|\Psi^-_{LX}\rangle \langle \Psi^-_{LX}| + |\Psi^-_{RX}\rangle \langle \Psi^-_{RX}| \right)}_{=1} |\Psi^+_{RX}\rangle \\ &= \langle \Psi^+_{RX} | \Psi^+_{RX} \rangle = 1 \\ a_{22} &= \langle \Psi^+_{LX} | \left(|\Psi^-_{LX}\rangle \langle \Psi^-_{LX}| + |\Psi^-_{RX}\rangle \langle \Psi^-_{RX}| \right) |\Psi^+_{LX}\rangle \\ &= \langle \Psi^+_{L,X} | \Psi^+_{LX} \rangle = 1 \\ a_{12} &= \langle \Psi^+_{RX} | \left(|\Psi^-_{LX}\rangle \langle \Psi^-_{LX}| + |\Psi^-_{RX}\rangle \langle \Psi^-_{RX}| \right) |\Psi^+_{LX}\rangle \\ &= \langle \Psi^+_{RX} | \Psi^+_{LX} \rangle = 0 \\ a_{21} &= \langle \Psi^+_{LX} | \left(|\Psi^-_{LX}\rangle \langle \Psi^-_{LX}| + |\Psi^-_{RX}\rangle \langle \Psi^-_{RX}| \right) |\Psi^+_{RX}\rangle \\ &= \langle \Psi^+_{LX} | \Psi^+_{RX} \rangle = 0. \end{aligned}$$

We have used that the $|\Psi^-_{R/LX}\rangle$ form an orthonormal basis. To show that $\mathbf{S}_X \mathbf{S_X}^\dagger = 1$ goes the same way using hat the $|\Psi^-_{R/LX}\rangle$ form an orthonormal basis. This way we have prooven Eq. (2.6).

References

[1] Yaroslav M. Blanter and Yuli V. Nazarov. *Quantum Transport - Introduction to Nanoscience*. Cambridge University Pr., May 2009.

[2] Niels Bode, Silvia Viola Kusminskiy, Reinhold Egger, and Felix von Oppen. Current-induced forces in mesoscopic systems: A scattering-matrix approach. *Beilstein Journal of Nanotechnology*, 2012.

[3] Jorg P. Kotthaus Daniel R. Koenig, Eva M. Weig. Ultrasonically driven nanomechanical single-electron shuttle. *Nature Nanotechnology*, Aug 2008.

[4] W. Demtröder. *Experimentalphysik Band 2: Elektrizität und Optik, 5.Auflg.* Springer, 2009.

[5] C. B. Doiron, W. Belzig, and C. Bruder. Electrical transport through a single-electron transistor strongly coupled to an oscillator. *Phys. Rev. B*, Nov 2006.

[6] A. Erbe, C. Weiss, W. Zwerger, and R. H. Blick. Nanomechanical resonator shuttling single electrons at radio frequencies. *Phys. Rev. Lett.*, Aug 2001.

[7] H. B. Meerwaldt, G. Labadze, B. H. Schneider, A. Taspinar, Ya. M. Blanter, H. S. J. van der Zant, and G. A. Steele. Probing the charge of a quantum dot with a nanomechanical resonator. *Phys. Rev. B*, Sep 2012.

[8] M. Moskalets and M. Büttiker. Adiabatic quantum pump in the presence of external ac voltages. *Phys. Rev. B*, May 2004.

[9] Amir H. Safavi-Naeini, Jasper Chan, Jeff T. Hill, Thiago P. Mayer Alegre, Alex Krause, and Oskar Painter. Observation of quantum motion of a nanomechanical resonator. *Phys. Rev. Lett.*, Jan 2012.

[10] Mark Thomas, Torsten Karzig, Silvia Viola Kusminskiy, Gergely Zaránd, and Felix von Oppen. Scattering theory of adiabatic reaction forces due to out-of-equilibrium quantum environments. *Phys. Rev. B*, Nov 2012.